Received: Added at production | Revised: Added at production | Accepted: Added at production

DOI: xxx/xxxx

ARTICLE TYPE

Identification of the source of an interferer by comparison with known carriers using a single satellite

Ian Glendinning*[1] | Michael Nölle[1] | Christian Hausleitner[2] | Erwin Greilinger[2]

[1]DSS, AIT Austrian Institute of Technology GmbH, Vienna, Austria
[2]Space Systems, Atos Convergence Creators GmbH, Vienna, Austria

Correspondence
*Ian Glendinning, AIT Austrian Institute of Technology GmbH, Giefinggasse 4, 1210 Vienna, Austria. Email: ian.glendinning@ait.ac.at

We describe a method for identifying the source of a satellite interferer using a single satellite. The technique relies on the fact that the strength of a carrier signal measured at the downlink station varies with time due to a number of factors, and we use a quantum-inspired algorithm to compute a 'signature' for a signal, which captures part of the pattern of variation that is characteristic of the uplink antenna. We define a distance measure to numerically quantify the degree of similarity between two signatures, and by computing the distances between the signature for an interfering carrier and the signatures of the known carriers being relayed by the same satellite at the same time, we can identify the antenna that the interferer originated from, if a known carrier is being relayed from it. As a proof of concept we evaluate the performance of the technique using a simple statistical model applied to measured carrier data.

KEYWORDS:
interferer, identification, single satellite, quantum inspired, singular value decomposition

1 | INTRODUCTION

The increasing demand for satellite communication links has led to an increasing number of satellite signals, and to an increasing amount of uplink interference. The causes of this interference include the growth in the number of small ground terminals, low quality equipment, poor installations and maintenance, uplink personnel mistakes (human error), faulty equipment, incorrectly pointed antennas, adjacent satellite interference, terrestrial service interference, and sometimes intentional jamming [1,2]. Satellite operators are therefore increasingly interested in solutions not only for detecting interference, which is the main task of a satellite monitoring system, but also to identify its source.

The traditional approach is to geographically localize, or geolocate, the transmitting station of an interferer. However, most localization systems need to receive the interference signal via two adjacent satellites in order to perform geolocation [3,4,5,6,7], and there are a number of limitations associated with this approach:

- An adjacent satellite must be available that is equipped with transponder(s) receiving components of the interfering signal and a reference signal (same uplink frequency range, same polarization).
- The interference and reference signals need to have enough crosstalk energy between the primary and adjacent satellites to achieve a sufficient level of correlation.
- Accurate ephemeris data must be available for both satellites.
- The reference signal needs to be received from both satellites via transponders operating with the same physical local oscillators (LOs) as the transponders re-transmitting the interference signal.

- If the system is installed at only one earth station, the downlink signals of both satellites need to be receivable at this earth station (downlink beams of both satellites need to cover the measurement site location). If this is not possible (beams pointing to different locations) the system needs to be installed at different locations inside the beams.

- A region is identified in which the transmitter is likely to reside, but additional steps are often necessary to actually identify the transmitter.

Geolocation can also be performed using crosstalk measurements between signals received from multiple antennas/beams belonging to the same satellite [8,9], but this approach has the drawback that additional payload resources are needed (antennas, transponders) or that operations must be interrupted to release resources. It has also been shown that frequency measurements of signals from a single satellite, taken at different times, can be used to locate an unknown emitter [10,11], but this approach is extremely susceptible to frequency instability introduced by the uplink terminal, which leads to very high localization errors unless the terminal's frequency stability is better than $\pm 1 \times 10^{-12}$ per day, which can be achieved for example via synchronization with a Galileo/GPS/GNNS disciplined frequency reference oscillator.

Here we describe a method able to identify the source of an interferer using a single satellite, based on the variation of signal strength with time, measured at the downlink station. It is a variant on a method that is the subject of Austrian patent [12] and of international, US, and European patent applications [13,14,15]. The main benefit of our approach is that it enables identification of unknown RFI transmitters based only on measurements of power variations. This overcomes the constraints of the above methods. Even in the case that the position of the transmitter of a 'matching' reference signal is not known, the result can be used for resolving the interference case by contacting the satellite operator's accounting department to get in touch with the customer (the individual operating the uplink) who is potentially causing the interference.

The main limitation of the approach is that the interferer must be from a known antenna from which a known carrier is also being relayed. This means that the method only works for antennas that are transmitting at least two carriers, and that the interferer must be from a known antenna. As an example, in 2018 roughly 30% of antennas pointing to a big satellite fleet transmitted two or more carriers, and in 2012 Türksat reported that just 3% of interference was due to unknown carriers [2], so our method is applicable in a significant number of cases. It is not a substitute for the traditional geolocation approach with adjacent satellites (based on TDOA/FDOA measurements), but in the case that the traditional approach does not work (no adjacent satellite available; different beam coverage; not the same uplink frequency; etc.), which happens more than 60% to 70% of the time, it offers an additional possibility.

The rest of this paper is structured as follows. Section 2 outlines our method and discusses the power variations that it relies on, and the limitations of the approach, as well its quantum-inspired aspects. In section 3 we explain in detail how to compute the signature, and in section 4 how to quantify the similarity between signatures. Section 5 analyses the performance of the method, and section 6 concludes.

2 | METHOD

Our method relies on the fact that the signal strength of a carrier that is measured at the downlink station varies with time due to a number of factors, and the technique is capable of identifying the antenna that an interferer originated from if another 'known' carrier is being relayed by the satellite at the same time from the same antenna. It turns out that there are similarities in the patterns of variation of signal strength for carriers originating from the same uplink antenna, and we found we were able to compute a 'signature' for the variation of signal strength for each carrier, that captures part of the pattern of variation that is characteristic of the uplink antenna.

In order to numerically quantify the degree of similarity or difference between two signatures, we compute a 'distance' between them, which is a number between 0 and 1. If the distance is close to zero, the signatures are similar (if they are identical the distance is zero), and if it is close to one, they are very different. This distance between signatures turns out to be lower on average for carriers from the same antenna than for carriers from different antennas, and by comparing the signature for an interfering carrier with the signatures for the other carriers being relayed by the same satellite, we can rank them according to their degree of similarity.

The causes of power variations in a received carrier include:

- Power variations from signal-sending hardware (satellite modem, frequency converter, power amplifier, etc.)

- Satellite movement versus antenna pattern and pointing mechanism (antenna tracking the satellite position or constant bearing towards the satellite, antenna pointing variations due to wind)

- Atmospheric losses due gases and hydrometeors

- Faraday rotation in the ionosphere

- Noise contributions (terrestrial noise picked up from the surface of the earth, receiver noise in both satellite and Rx ground station, atmospheric noise, extra-terrestrial noise from the sun and moon, etc.)

Our approach only works if the signal power is not strongly affected by the satellite transponders, so it applies to transparent transponders working with constant gain (fixed gain mode) and which are not saturated. In the case of saturation and/or if Automatic Level Control (ALC) is applied, the sensitivity of the measurements can be severely reduced, requiring different measurement settings (high averaging) and a reference carrier that is affected by the same mode of transponder operation in order for the approach to work. It does not work with regenerative transponders. The method works well with different transponders. A small reduction in similarity is introduced by frequency dependency, meaning that if a carrier's frequency is different by e.g. 1 GHz (Ku-Band) the level of similarity in power fluctuation is slightly reduced. More degradation of level of similarity comes from different polarization, but the similarity is still high enough for successful detection.

The sensitivity of the measurement could perhaps be increased if downlink path influences, such as the power variation of a beacon signal and/or the transponder noise floor and/or the average power variation of all the signals on the downlink, were subtracted from the unknown signal and the known signal.

2.1 | A quantum-inspired algorithm

The algorithm we present here to calculate the similarity between two carriers is based on the one described in the patent applications [12,13,14,15], which is a so-called 'quantum inspired algorithm', in which concepts from quantum information theory are applied to the representation and processing of classical information [16,17,18]. The first step in developing a quantum inspired algorithm is to find a suitable encoding of the information as quantum states, which can then be manipulated using the well-developed mathematical techniques of quantum information theory. In the patent applications the signal was encoded in terms of qubits (quantum bits), which has advantages when the absolute value of the signal contains significant information, but in this case we subtract a running average from it, so there is no advantage in using the qubit encoding. In the qubit representation each signal value is mapped to two values in a vector that is normalized to have an ℓ_2 norm (Euclidean norm) of 1, but here we map each signal value to a single value in a normalized vector. Both kinds of vector are valid representations of quantum states in a Hilbert space[1]. In the patent application we used the Schmidt decomposition [19,20] to analyse the 24-hour periodic structure of the signal, and to extract its principal components [21], one of which served as a 'signature', and we defined a distance measure. Here we use the singular value decomposition, which is equivalent to the Schmidt decomposition, together with the same distance measure.

Although the algorithm presented here was inspired by concepts from quantum information theory, we have expressed it in terms of a finite-dimensional inner product space and the singular value decomposition, which are familiar concepts in statistical signal processing.

3 | COMPUTING THE SIGNATURE

The signature is computed from a sequence of satellite downlink EIRP (Equivalent Isotropically Radiated Power) values representing the variation from the uplink signal, measured in dBW, calculated as follows:

$$\mathrm{EIRP}[\mathrm{dBW}] = \mathrm{P_{sa}}[\mathrm{dBm}] + \mathrm{L_{fs}}[\mathrm{dB}] - \mathrm{G_{ant}}[\mathrm{dB}] - \mathrm{G_{path}}[\mathrm{dB}] - 30\mathrm{dB}, \tag{1}$$

where $\mathrm{P_{sa}}$ is the power at the input of the monitoring device (Spectrum Analyzer), $\mathrm{L_{fs}}$ is free space loss, $\mathrm{G_{ant}}$ is the receiving antenna gain, $\mathrm{G_{path}}$ is the path gain from the antenna feed to the spectrum analyzer, and $30\mathrm{dB}$ is the conversion from dBm to dBW. The measurement process takes into account the contribution of noise when calculating $\mathrm{P_{sa}}$, subtracting it from the received signal (power + noise). The SNR limitation of this process is about 3 dB, meaning that signals with SNR below 3 dB are not taken into account. This limit is chosen in order to keep the additional error due to estimation and subtraction of noise small. If noise was not subtracted, the measurement would suffer from sensitivity in terms of reduced amplitude of power fluctuations

The EIRP values must be equally spaced in time, so if the raw data was not measured at a fixed time interval, it must be interpolated to give values that are equally spaced in time. The data used for the results presented in this paper was interpolated at three minute intervals, which was roughly half the average interval between measurements in the raw data. For the calculation of the signature it is the variation of the EIRP with time is important rather than its absolute value, so the absolute value is removed in following steps.

3.1 | Expressing EIRP values as a state vector

Given a vector of EIRP values $(\mathrm{EIRP}_1, \mathrm{EIRP}_2, \ldots, \mathrm{EIRP}_\mathrm{i}, \ldots, \mathrm{EIRP}_\mathrm{N})$ corresponding to times $\mathrm{t}_1, \mathrm{t}_2, \ldots, \mathrm{t}_\mathrm{i}, \ldots, \mathrm{t}_\mathrm{N}$, with equal intervals between them, we first subtract a running average from the EIRP values, using a window of a specified width in time. This has the effect that constant

[1] Although here we are working with vectors in a real inner product state, which is a special case of a Hilbert space, this approach can be generalized to use complex vectors, as explained in [12,13,14,15]

differences between the average EIRP values of two carriers, which are not relevant to the signature, are not taken into account. To generate the results presented here, we used a Gaussian window with a standard deviation of 6 hours, meaning that average differences between one day and the next were also removed, and we call the resulting values $\mathbf{E} = (\mathsf{E}_1, \mathsf{E}_2, \ldots, \mathsf{E}_\mathsf{i}, \ldots, \mathsf{E}_\mathsf{N})$.

Now, for our quantum-inspired algorithm we wish to encode these values as a quantum state vector, which we call

$$\mathbf{q} = (q_1, q_2, \ldots, q_i, \ldots q_N). \tag{2}$$

To qualify as a state vector $\mathbf{q}$ must have a norm of one [20], i.e. $\|\mathbf{q}\| = 1$, where for the special case of a quantum state for which all of the q_i are real numbers the norm is defined as

$$\|\mathbf{q}\| = \sqrt{\mathbf{q}^\mathsf{T}\mathbf{q}}. \tag{3}$$

This means that $\mathbf{q}^\mathsf{T}\mathbf{q} = \sum_\mathsf{i} \mathsf{q}_\mathsf{i}^2 = 1$, and the q_i^2 values can be interpreted as probabilities because they are between 0 and 1 and their sum is one. In quantum mechanics the q_i values are known as (probability) amplitudes and the q_i^2 values correspond to the probabilities of particular outcomes of measurements. It is the amplitudes that are the fundamental quantities, so we choose to encode the signal in terms of them. We first define

$$e_i = \frac{E_i + E_{max}}{2E_{max}}, \tag{4}$$

where E_max is the maximum absolute value of E_i for all i, that is, $\mathsf{E}_\mathsf{max} = \max_\mathsf{i} |\mathsf{E}_\mathsf{i}|$, so that $0 \leq \mathsf{e}_\mathsf{i} \leq 1$. We then let[2]

$$p_i = \frac{e_i}{\sum_j e_j}, \tag{5}$$

so that the p_i values form a valid probability distribution, with $0 \leq \mathsf{p}_\mathsf{i} \leq 1$ and $\sum_\mathsf{i} \mathsf{p}_\mathsf{i} = 1$, and we derive our q_i values from the p_i values, by defining $\mathsf{q}_\mathsf{i}^2 = \mathsf{p}_\mathsf{i}$, so that

$$q_i = \sqrt{p_i}, \tag{6}$$

taking the positive square root, so that $0 \leq \mathsf{q}_\mathsf{i} \leq 1$.

It might be thought that it would be simpler to encode the data as a state vector by defining $\mathbf{e} = (\mathsf{e}_1, \mathsf{e}_2, \ldots, \mathsf{e}_\mathsf{i}, \ldots \mathsf{e}_\mathsf{N})$ and $\mathbf{r} = \mathbf{e}/\|\mathbf{e}\|$, thus avoiding the square root in equation 6, but although $\mathbf{r}$ is a valid state vector, we found that the 'quantum-inspired' approach of encoding the data as probability amplitudes in $\mathbf{q}$ gave slightly better results in terms of being able to distinguish between pairs of carriers from the same antenna and from different antennas when using the distance measure defined in section 4.

3.2 | Generating 'eigensignals' for a state vector

Geostationary satellites are not completely stationary relative to stations on the ground, moving north-south and east-west due to their orbital inclination, eccentricity, and longitude drift. This leads to a 24-hour variation in the signal strength at the receiving station, which can be seen in the plots of q_i in figures 1 and 2. It is also present in q_i signals plotted in figures 3 and 4, though it is not as obvious in those plots. We use the singular value decomposition to generate 'eigensignals' for state vectors, based on this 24-hour periodicity.

We consider EIRP data for m days, with n values per day, $\mathbf{E} = (\mathsf{E}_1, \mathsf{E}_2, \ldots \mathsf{E}_\mathsf{N})$, where $\mathsf{N} = \mathsf{mn}$, and express the values as a state vector $\mathbf{q}$ using equations 4, 5, and 6, then we define the Matrix $\mathbf{M}$ in terms of the elements of $\mathbf{q}$ to be

$$\mathbf{M} = \begin{pmatrix} \mathsf{q}_1 & \mathsf{q}_2 & \cdots & \mathsf{q}_\mathsf{n} \\ \mathsf{q}_{\mathsf{n}+1} & \mathsf{q}_{\mathsf{n}+2} & \cdots & \mathsf{q}_{2\mathsf{n}} \\ \mathsf{q}_{2\mathsf{n}+1} & \mathsf{q}_{2\mathsf{n}+2} & \cdots & \mathsf{q}_{3\mathsf{n}} \\ \vdots & \vdots & & \vdots \\ \mathsf{q}_{(\mathsf{m}-1)\mathsf{n}+1} & \mathsf{q}_{(\mathsf{m}-1)\mathsf{n}+2} & \cdots & \mathsf{q}_{\mathsf{mn}} \end{pmatrix}, \tag{7}$$

so that each row corresponds to data from one day. Taking the singular value decomposition (SVD) of $\mathbf{M}$, we can write:

$$\mathbf{M} = \mathbf{U}\mathbf{S}\mathbf{V}^T, \tag{8}$$

where $\mathbf{U}$ is an $\mathsf{m} \times \mathsf{m}$ orthogonal matrix, $\mathbf{S}$ is an $\mathsf{m} \times \mathsf{n}$ diagonal matrix containing non-negative real numbers, and $\mathbf{V}$ is an $\mathsf{n} \times \mathsf{n}$ orthogonal matrix. The columns of $\mathbf{V}$ are called the right-singular vectors of $\mathbf{M}$, and they are orthonormal and are the principal components of the rows of $\mathbf{M}$. We refer to them as $\mathbf{v}_\mathsf{i}$, and they characterize features of the signal over 24-hour periods. As they are the eigenvectors of the covariance matrix $\mathbf{M}^\mathsf{T}\mathbf{M}$, we call them 'eigensignals'. In a celebrated paper [22] this technique was applied to the classification of human faces. The diagonal entries s_i of $\mathbf{S}$ are known as the singular values of $\mathbf{M}$, and they are ordered so that s_1 is the largest, and they decrease with increasing i, so the $\mathbf{v}_\mathsf{i}$ vectors with small

[2] We could have defined p_i directly in terms of $\mathsf{E}_\mathsf{i} + \mathsf{E}_\mathsf{max}$, but we find it clearer to introduce e_i as an intermediary

values of i make the greatest contribution to the signal. The columns of $\mathbf{U}$ are the left-singular vectors of $\mathbf{M}$, and they contain the information on the proportion of each eigensignal that is present in the signals for each day.

The $\mathbf{v}_1$ vector picks out the dominant part of the 24-hour variation in the signal, which turns out not to be very characteristic of the uplink antenna, and to be rather similar for all carriers sharing the same downlink. However, the $\mathbf{v}_2$ vector is characteristic of the uplink antenna, and we therefore use $\mathbf{v}_2$ as the signature. Figure 1 shows q_i and $\mathbf{v}_2$ for a carrier transmitted from an antenna at a station in Rugby (England) over the 31 days in December 2012, and figure 2 shows the corresponding plots for another carrier transmitted from the same antenna in Rugby during the same period. As can be seen, the $\mathbf{v}_2$ values are very similar to each other. For comparison, figures 3 and 4 show the corresponding plots for two carrier signals from an antenna in Mińsk Mazowiecki (Poland) during the same period, and again the $\mathbf{v}_2$ values are very similar to each other, but quite different to the ones for the signals from the antenna in Rugby.

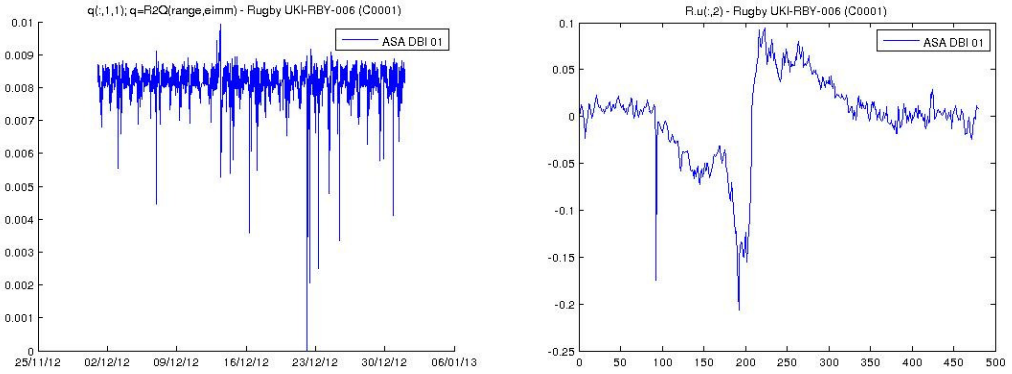

FIGURE 1 q_i vs i (left) and $\mathbf{v}_2$ (right), for a signal from Rugby

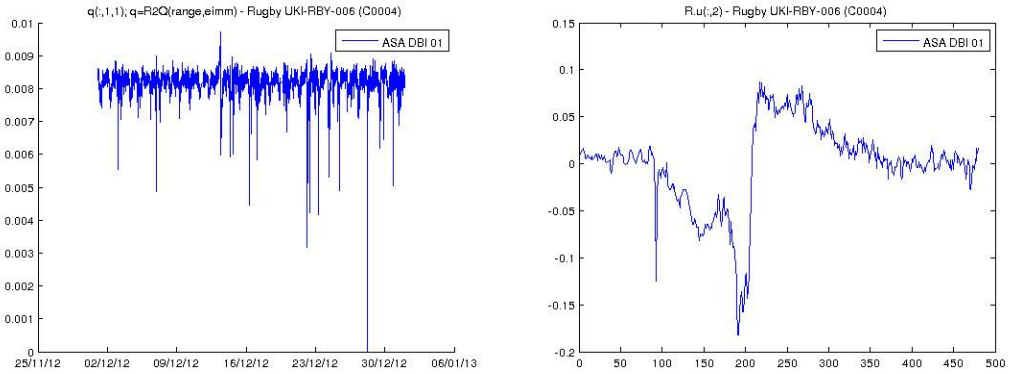

FIGURE 2 q_i vs i (left) and $\mathbf{v}_2$ (right), for a second signal from Rugby

4 | QUANTIFYING THE SIMILARITY BETWEEN SIGNATURES

The scalar product of two vectors $\mathbf{r}$ and $\mathbf{s}$ with real components is $\mathbf{r}^{\mathrm{T}}\mathbf{s}$ and if they have a norm of one we can use this to define a measure D of the distance between them,

$$D(\mathbf{r},\mathbf{s}) = \sqrt{1 - |\mathbf{r}^T\mathbf{s}|^2}, \tag{9}$$

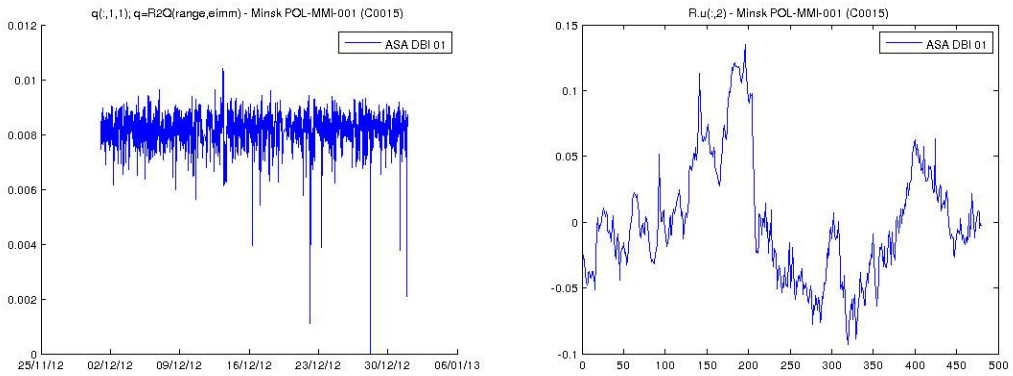

FIGURE 3 q_i vs i (left) and $\mathbf{v}_2$ (right), for a signal from Mińsk Mazowiecki

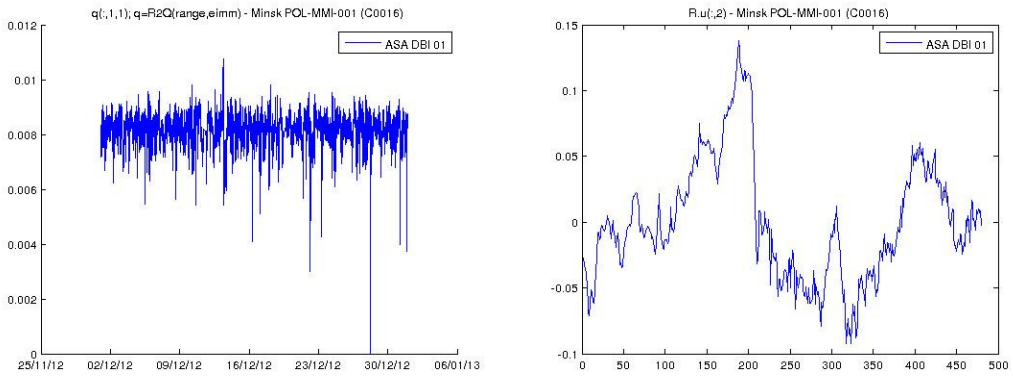

FIGURE 4 q_i vs i (left) and $\mathbf{v}_2$ (right), for a second signal from Mińsk Mazowiecki

which is zero when the vectors are identical, and is one when they are maximally different (orthogonal). Since the $\mathbf{v}_i$ vectors from the SVD are orthonormal, the signatures, $\mathbf{v}_2$, have a norm of one, and we use D to calculate the distance between pairs of them, to quantify their similarity. The distance for carriers from the same antenna turns out to be lower on average than for carriers from different antennas.

5 | PERFORMANCE EVALUATION

In order to quantitatively test this approach for identifying signals we developed a statistical model based on histograms of distances between carriers, and applied the model to carrier data that was monitored in Dubai in December 2012, consisting of 53 carriers from 32 antennas, which were relayed by the SESAT2 satellite. The data collected at Dubai was chosen because of its high quality, with data that was sampled at a relatively constant rate, and with a single monitoring device. Some of the other data that was available to us suffered from a sampling rate that was patchy, and it was collected with multiple monitoring devices operating in a round-robin fashion, which meant that the sampling rate for each monitoring device was realtively low. We initially analysed the Dubai data from the whole month, and then investigated the performance for shorter periods of time. We subsequently analysed data that was monitored at other sites, and found that the performance depended on the satellite and on the interval between measurements in the raw data. For comparison with the results for the Dubai data, we give results for data that was monitored at Rambouillet (the site was actually called Rambouillet_2) during the same time period, consisting of 85 carriers from 51 antennas, which were relayed by the E10A satellite.

5.1 | Statistical model and results for data from Dubai for one month

Figure 5 shows the frequency distributions of distances between pairs of different carriers, from the same antenna, $f_s(D)$, and from different antennas, $f_d(D)$, using data for each carrier for the whole month. For the 53 carriers there are $\binom{53}{2} = 53 \times 26 = 1378$ pairs, 70 of which were from the same antenna, and 1308 of which were from different antennas. It can be seen that the distances between most carriers from the same antenna are much lower than the distances between carriers from different antennas, so fairly good separation can be obtained between carrier pairs from the same antenna and pairs from different antennas.

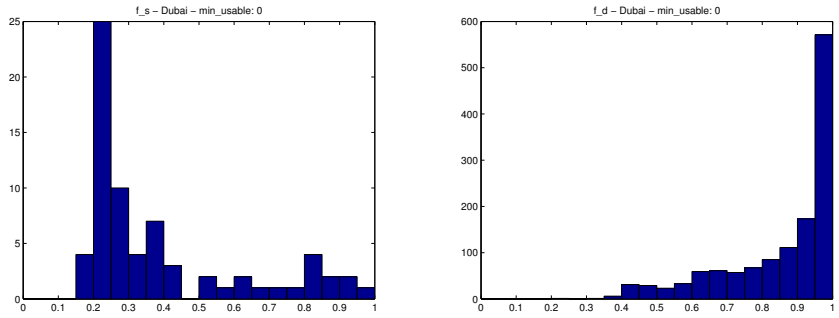

FIGURE 5 $f_s(D)$ (left) and $f_d(D)$ (right) - Dubai

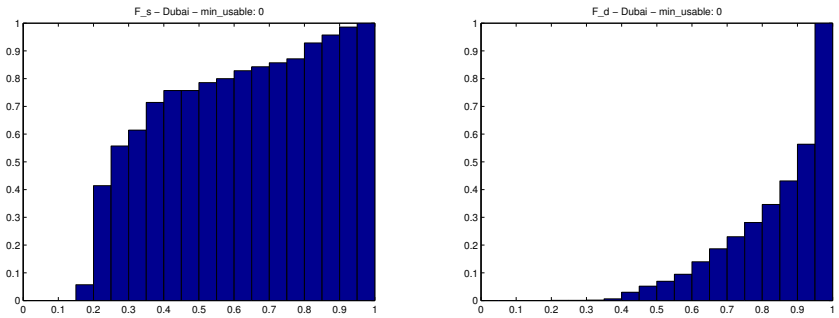

FIGURE 6 $F_s(D)$ (left) and $F_d(D)$ (right) - Dubai

The quality of the separation can be characterized using the corresponding relative cumulative frequency distributions, for pairs of carriers from the same antenna, $F_s(D)$, and from different antennas, $F_d(D)$, shown in figure 6. $F_s(D)$ is an estimate of the probability that the distance between a pair of carriers from the same antenna is less than D. For example, the value of $F_s(0.4)$ is approximately 0.71. Given the scenario that an interfering carrier is coming from one of a number of known uplink antennas, but we don't know which one, our approach for identifying the antenna is to calculate the distances from the interferer to all the known carriers from the satellite that is relaying the interferer, and to select those for which the distance D is less than a specified threshold D_t, and we refer to those carriers as being in the 'result set'. $F_s(D_t)$ is therefore an estimate of the probability that a given carrier from a satellite is in the result set. Each carrier in the result set that is from the same antenna as the interferer is a positive identification of the source of the interferer, so we refer to these as positives. The result set can also contain carriers that are not from the same antenna as the interferer, which we refer to as false positives. In what follows we analyse the probabilities of obtaining at least one positive and at least one false positive, and the expected number of positives and of false positives, averaged over all antennas, and we also consider the influence of the number of carriers per antenna.

5.1.1 | Probability of at least one positive

Typically several carriers are transmitted from the same antenna at the same time, so the probability that at least one carrier from the same antenna as the interferer is in the result set is bigger than $F_s(D_t)$, because $F_s(D_t)$ is a probability estimate for a single pair, but on average there is more than one of them. We call this probability p_{id}, because it is the probability that at least one carrier has been correctly identified as coming from the same antenna as the interferer. For each known carrier, the probability that it is not in the result set is $1 - F_s(D_t)$, so for an antenna with K carriers the probability that none of them are in the result set is $(1 - F_s(D_t))^K$. If the number of antennas that have K carriers is $n(K)$, then averaged across antennas, the probability that none of the carriers are in the result set, which we call $\bar{p}_{id}$, is

$$\bar{p}_{id} = \frac{\sum_K n(K)(1 - F_s(D_t))^K}{\sum_K n(K)}. \tag{10}$$

Now, the sum in the denominator of this equation is equal to the total number of antennas, which we call N_a and the probability that at least one carrier in the result set came from the same antenna as the interferer is $1 - \bar{p}_{id}$, so

$$p_{id} = 1 - \frac{1}{N_a} \sum_K n(K)(1 - F_s(D_t))^K. \tag{11}$$

Table 1 shows $n(K)$ For the Dubai data in December 2012, and if we choose $D_t = 0.4$ for our threshold, for which $F_s(D_t) = 0.714$, the probability that the antenna we are seeking is in the result set is approximately $p_{id} = 0.76$. Table 1 also shows the number of same-antenna pairs for each value

TABLE 1 n(K) and the number of same-antenna pairs for Dubai data in December 2012

K	n(K)	same-antenna pairs
1	27	0
2	1	1
3	1	3
6	2	30
9	1	36

of K, and it can be seen that 66 out of the population of 70 same-antenna pairs come from just three antennas, and all 70 of the pairs come from five antennas out of the total of 32 antennas. Furthermore, 351 of the different-antenna pairs are drawn from a completely different population to those used for the same-antenna carrier comparisons, and 1053 of the different antenna carrier comparison involve at least one of the antennas in a different population to those used for the same antenna carrier comparisons. For comparison, the data from Rambouillet, which is presented in section 5.4, has a larger proportion of antennas with more than one carrier.

5.1.2 | Expected number of positives

We call the expected number of positives n_i, because they are carriers that have been correctly identified as coming from the same antenna as the interferer, and we call the average number of carriers per antenna n_s, because it is the average number of carriers from the same antenna. Only carriers from the same antenna as the interferer can contribute towards n_i, and on average there will be n_s of them. We can consider the decision as to whether the distance of each of these carriers from that of the interferer is less than D_t as being independent trials, so the probability that a carrier from the same antenna as the interferer is in the result set (the trial is a success) is equal to the number of successes n_i divided by the number of trials n_s, but we know that this probability is given by $F_s(D_t)$, so we have $F_s(D_t) = n_i/n_s$, which gives an estimate for n_i of

$$n_i = n_s F_s(D_t). \tag{12}$$

A more detailed analysis takes into account the distribution of the number of carriers per antenna. We can consider the decisions as to whether the distances between each carrier from the antenna and the interferer are less than D_t as being independent trials, so the probability of obtaining k positives from an antenna with K known carriers, which we call $P(k)$, will follow a binomial distribution, and if we let $p = F_s(D_t)$ and $q = 1 - p$, then

$$P(k) = \binom{K}{k} p^k q^{K-k}. \tag{13}$$

The expected value of k is known to be

$$\bar{k} = \sum_k kP(k) = Kp, \tag{14}$$

and given the distribution $n(K)$, and averaging over K, the expected number of positives is

$$n_i = \langle \bar{k} \rangle = \frac{p}{N_a} \sum_K n(K)K = \bar{K}p, \tag{15}$$

where $\bar{K} = n_s$, the average number of carriers from the same antenna, so we obtain the same result as equation 12.

For the Dubai data in December 2012 the value of n_s was approximately 1.66 and $F_s(0.4)$ was 0.71, so n_i is therefore approximately 1.2.

5.1.3 | Expected number of false positives

In general the result set will also contain some carriers from antennas other than the one that we are trying to identify, and the number of such false positives, which we call n_f, can be estimated using $F_d(D)$, which is an estimate of the probability that the distance between a pair of carriers from different antennas is less than D. A similar argument to the one that led to equation 12 gives

$$n_f = n_d F_d(D_t), \tag{16}$$

where n_d is the number of carriers from different antennas to the one that the interferer originated from. We call the number of carriers relayed by the satellite is N_s, and we know that of these, on average n_s of them are from one particular antenna, so the average the number that are from other antennas is

$$n_d = N_s - n_s, \tag{17}$$

so we have

$$n_f = (N_s - n_s)F_d(D_t), \tag{18}$$

For this example case, 53 carriers were relayed by the satellite, so $N_s = 53$, and given our example threshold of $D_t = 0.4$, the value of $F_d(0.4)$ is approximately 0.0061, so we have an estimated number of $n_f = n_d F_d(D_t) = 51.34 \times 0.0061$ false positives, which is approximately 0.31. Note that a slightly higher value of D_t, say $D_t = 0.5$, would give a higher expected number of positives, of $n_i = 1.25$, but also a much higher number of false positives, $n_f = 2.7$.

Note also that we need not restrict our data to carriers relayed by the same satellite as the interferer, since other satellites may also relay carriers from the antenna that is the source of the interferer, but it was found that for the data at our disposal, including such carriers increased the false positive rate significantly, with little or no increase in the number of positives.

5.1.4 | Probability of one or more false positives

For a carrier from an antenna with K carriers there are $N_s - K$ possible comparisons with carriers from the other antennas, and if we now let $p = F_d(D_t)$ then the probability of one or more false positives, which we call p_f^K, as it applies to an antenna with K carriers, is

$$p_f^K = 1 - (1-p)^{(N_s - K)}. \tag{19}$$

Provided p is small, this approximates to

$$p_f^K \simeq (N_s - K)p, \tag{20}$$

which happens to also equal the expected number of false positives for that antenna, which we call n_f^K. Provided N_s is large and K is small, (20) is not a strong function of K, and with this assumption

$$p_f^K = n_f^K \simeq N_s p \simeq \langle p_f^K \rangle = \langle n_f^K \rangle, \tag{21}$$

and this would be the expected result averaged over all the antennas, which we call $p_f = \langle p_f^K \rangle$, and we have

$$p_f \simeq N_s p = N_s F_d(D_t), \tag{22}$$

For the Dubai data in December 2012 the probability of one or more false positives is therefore approximately $p_f = 0.32$.

5.1.5 | The influence of the number of carriers per antenna

So far we have considered probabilities and expectation values averaged over all the antennas relayed by the satellite, which gives some idea of the performance of our approach, independent of the interferer. However, once the result set has been calculated for a particular interferer, there is extra information available, as we know which antennas the carriers in the result set came from, and how many known carriers are being transmitted by those antennas, and that can be taken into account in interpreting the results.

If the interferer came from an antenna transmitting K carriers, the probability of obtaining k positives in the result set is given by equation 13, where $p = F_s(D_t)$ and $q = 1 - p$, and the same equation gives the probability of obtaining k false positives, if we define $p = F_d(D_t)$. In the above example for the data from Dubai we have $F_s(D_t) = 0.714$ and $F_d(D_t) = 0.0061$ and, for example, in the case of nine carriers per antenna, the

probability of obtaining a single positive is 0.000288, whereas the probability of obtaining a single false positive is 0.052. Therefore, in the case of a single carrier in the result set from an antenna with nine carriers, it is much more likely to be a false positive than a positive. The expected number of positives is given by equation 14, which in this case is 6.4, and the low probability of a single positive reflects the fact that one carrier is much less than this expected value.

On the other hand, for the same antenna with nine carriers, the probability of three positives is 0.0167, whereas the probability of three false positives is 1.83×10^{-5}. Therefore if there are three carriers in the result set from an antenna with nine carriers they are much more likely to be positives than false positives.

Similarly, with a three-carrier antenna, the probability of the result set containing a single positive if the interferer came from that antenna is 0.175, whereas the probability of a single false positive is 0.018, so in this case a single carrier in the result set is more likely to be a positive than a false positive, which reflects the fact that one positive is closer to the expected number of positives (which is 2.14) than for the case of the nine-carrier antenna.

5.2 | Results for data from Dubai for two days

So far we have presented data from a period of one month, but we also tried analysing data from shorter periods of time, and found that results with $n_i > n_f$ could be obtained for periods right down to two days, which was the minimum amount of data necessary for the algorithm to work in its original form. However, we found that the results were better for some two-day periods than for others. This can be seen from figures 7 and 8, which show the frequency distributions of distances between pairs of carriers from the same antenna, $f_s(D)$, and from different antennas, $f_d(D)$, for data monitored by Dubai for two different two-day periods in December 2012. Note that the number of counts in figure 7 (left) is roughly twice that of figure 8 (left), which is because not all carriers were present for the whole month, and for each period, only carriers were considered that were present for the whole of the period. The data in figure 7 is for pairs taken from 68 carriers, and in figure 8 it is from 54 carriers. The average number of carriers per antenna was also higher for the data in figure 7, which further boosted the number of pairs.

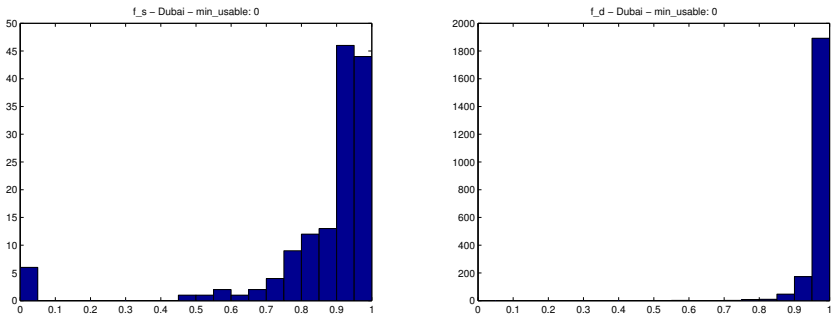

FIGURE 7 $f_s(D)$ (left) and $f_d(D)$ (right) - Dubai, 1-2 Dec. 2012

The best separation is shown by the data from 15-16 December 2012, for which a choice of $D_t = 0.7$ gives $p_{id} = 0.64$, $n_i = 0.97$, $n_f = 0.19$, and $p_f = 0.20$.

5.3 | Results for data from Dubai for less than two days

The algorithm was designed to require a minimum of two days of data (two periods of 24 hours each), as it compared one day with the next, in order to remove the 24 hour variation that is present in all carriers, and all of the results presented in the previous sections used that version of the algorithm. We then decided to investigate whether the algorithm could still identify characteristic features of carriers if it was modified to use periods of less than 24 hours, which would mean that the 24 hour variation was not removed. The modified algorithm still compares data from equal-length periods, and there must be at least two of them, but they can be of arbitrary length, and in particular, less than 24 hours.

Figure 9 shows the frequency distributions of distances between pairs of carriers from the same antenna, $f_s(D)$, and from different antennas, $f_d(D)$, for one day's data, monitored at Dubai for December 15th 2012, split into two 12 hour periods. It can be seen that there is some separation

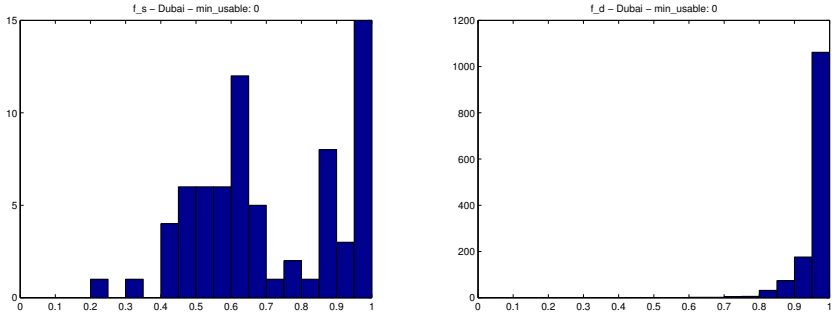

FIGURE 8 $f_s(D)$ (left) and $f_d(D)$ (right) - Dubai, 15-16 Dec. 2012

between carrier pairs from the same antenna and pairs from different antennas, and choosing $D_t = 0.85$ gives $p_{id} = 0.62$, $n_i = 0.93$, $n_f = 0.92$, and $p_f = 0.95$.

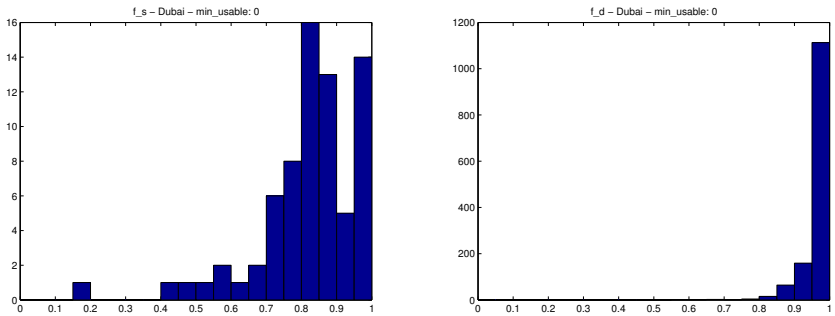

FIGURE 9 $f_s(D)$ (left) and $f_d(D)$ (right) - Dubai, 15 Dec. 2012

Figure 10 shows the frequency distributions of distances between pairs of carriers from the same antenna, $f_s(D)$, and from different antennas, $f_d(D)$, for half a day's data, monitored at Dubai for the first 12 hours of December 15th 2012, split into two 6 hour periods. Again it can be seen that there is some separation between carrier pairs from the same antenna and pairs from different antennas, and choosing $D_t = 0.85$ gives $p_{id} = 0.33$, $n_i = 0.33$, $n_f = 0.69$, and $p_f = 0.71$.

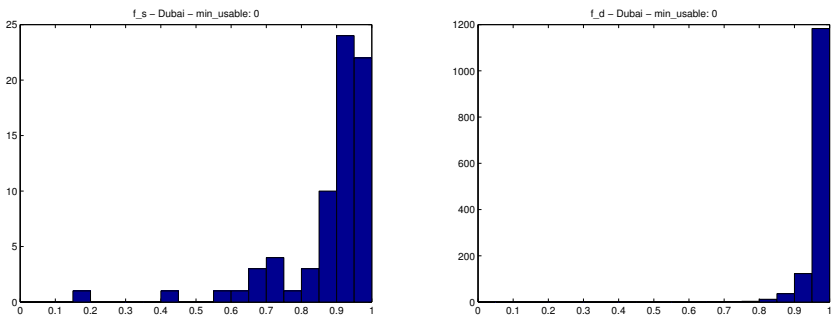

FIGURE 10 $f_s(D)$ (left) and $f_d(D)$ (right) - 0:00–12:00, Dubai, 15 Dec. 2012

It is encouraging that the algorithm works at all for less than one day's data, and although the results presented here show that it works less well for shorter periods, this is based on a fixed sampling rate of EIRP values, meaning that the shorter periods contain less data. As long as the signal contains enough structure, a higher sampling rate should give better results.

5.4 | Results for data from Rambouillet

Unlike in Dubai, where there was a single monitoring device, the data from Rambouillet was collected by four monitoring devices that operated in a round-robin fashion, which meant that some modification to our algorithm was necessary. Because the characteristics of some of the monitoring devices differed markedly. e.g. in sensitivity, it was decided not to interleave the recorded data values in a time-ordered sequence, because there could be big jumps between adjacent values. Instead, the blocks of data for each monitoring device were contatentated. That is, after interpolation of the data to create N values for each monitoring device, the N values for the second monitoring device were appended to those for the first monitoring device, and the N values for the third monitoring device were then appended, and so on, to create a sequence of values of length 4N, which was then analysed as if it had come from a single monitoring device.

Figure 11 shows the frequency distributions of distances between pairs of different carriers, from the same antenna, $f_s(D)$, and from different antennas, $f_d(D)$, for data that was monitored at Rambouillet (actually Rambouillet_2) during the whole of December 2012. It can be seen that, unlike in the case of the Dubai data, some of the same-antenna carrier pairs have high distances, so the separation between same-antenna pairs and different-antenna pairs is not as good. Table 2 shows $n(K)$ and the number of same-antenna pairs for each value of K for this data, and if we choose

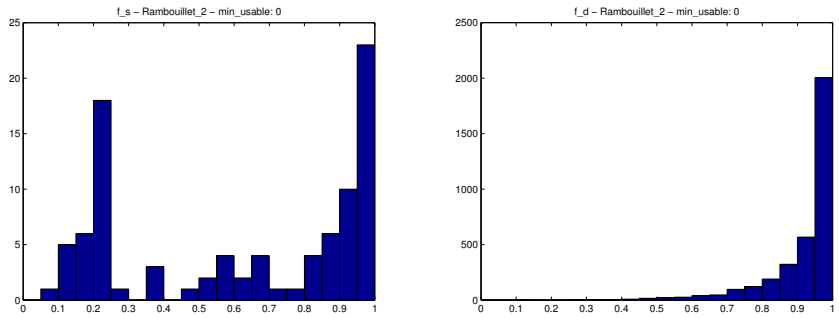

FIGURE 11 $f_s(D)$ (left) and $f_d(D)$ (right) - Rambouillet, December 2012

$D_t = 0.5$ for our threshold, for which $F_s(D_t) = 0.380$, we obtain $p_{id} = 0.48$, $n_i = 0.63$, $n_f = 0.91$, so in this case the expected number of false positives is about fifty percent more than the expected number of positives. The assumption we made of a low p value for our estimate of p_f does not hold in this case, so we do not give a value for it.

TABLE 2 n(K) and the number of same-antenna pairs for Rambouillet data in December 2012

K	n(K)	same-antenna pairs
1	36	0
2	9	9
3	3	9
5	1	10
8	1	28
9	1	36

Figure 12 shows the frequency distributions $f_s(D)$ $f_d(D)$ for data from the two-day period of December 15-16, 2012. With a choice of $D_t = 0.8$ for our threshold, for which $F_s(D_t) = 0.413$, we obtain $p_{id} = 0.49$, $n_i = 0.66$, $n_f = 2.20$, so in this case the expected number of false positives is

over three times more than the expected number of positives. Again, the assumption we made of a low p value for our estimate of p_f does not hold in this case.

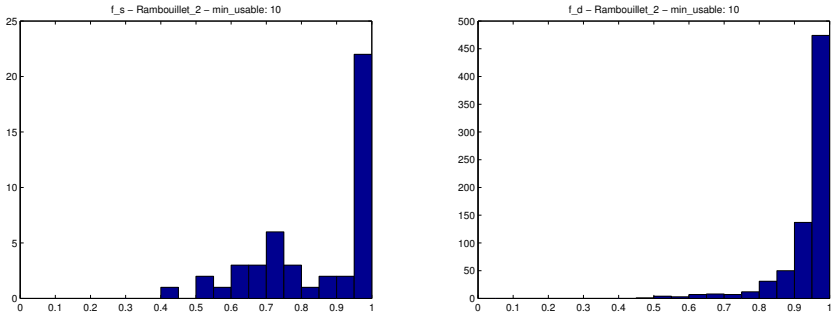

FIGURE 12 $f_s(D)$ (left) and $f_d(D)$ (right) - Rambouillet, 15-16 Dec. 2012

It should be noted that some of the carriers in the data from Rambouillet had a very small number of measurements for some monitoring devices for some days, and for that reason we required at least ten measurements per day per monitoring device for the two-day period. Without that constraint, the separation between same-antenna pairs and different-antenna pairs was much worse, and requiring more than ten measurements reduced the numbers of entries in the histograms to values that were considered to be too small to give meaningful results.

6 | CONCLUSION

We have described a method for identifying the source of a satellite interferer using a single satellite, which relies on the variation with time of the strength of carrier signals measured at the downlink station. The method uses a quantum-inspired algorithm to compute a signature for each carrier, and a distance between the signature for an interfering carrier and the signatures of all known carriers being relayed by the same satellite. As a proof of concept we have presented a simple statistical model to estimate the probability of successful identification of the source of an interferer, the expected number of carriers correctly identified to have originated from the interfering transmitter, the expected number of false positives, and the probability of one or more false positives, and we have used the model to evaluate the performance of the technique using measured data relayed by one satellite.

We initially analysed data for a sample of 53 carriers relayed by one satellite, which was sampled at a relatively constant rate, with a single monitoring device, and we have presented results using data for one month, and also for two days and less. In its original form the algorithm was designed to work with a minimum of two days' of data, and we found that the results were better for some two-day periods than others, but that in some cases successful identification was possible. We also modified the algorithm to operate on less than two days' of data, and we found that the results were less good, but that positive identification was still possible in some cases. However, the results were based on a fixed sampling rate, meaning that the shorter periods contained less data, and a higher sampling rate should give better results.

We subsequently analysed data monitored at sites where the sampling rate was less constant and multiple monitoring devices were used in a round-robin fashion, which meant that the sampling rate for each monitoring device was relatively low. We have presented results for a sample of 85 carriers monitored at such a site, relayed by a different satellite. The performance of the algorithm was less good, but we expect that a higher sampling rate would give better results.

ACKNOWLEDGMENTS

This work was supported by the Austrian Research Promotion Agency (FFG contract number 833427) and the European Space Agency (ESA/ESTEC contract number 4000109530/13/NL/US). We are indebted to Alexander Ploner for invaluable advice on the statistical analysis of the measured data, and to Thomas Zemen and Piotr Gawron for comments that greatly improved the manuscript.

References

1. Coleman M. Jamming overview. ITU Workshop on the efficient use of the spectrum/orbit resource, Limassol, Cyprus April 2014. URL https://www.itu.int/en/ITU-R/space/workshops/cyprus-2014/\Documents/Presentations/Martin%20Coleman%20-%20Jamming%20Overview.ppt.

2. Öz I. Harmful interference: regional security consequences. UNIDIR regional seminar: Building confidence for Eurasian space activities through norms of behaviour, Astana, Kazakhstan October 2013. URL http://www.unidir.ch/files/conferences/pdfs/harmful-interference-regional-\security-consequences-en-1-933.pdf.

3. Chestnut PC. Emitter location accuracy using TDOA and differential Doppler. *IEEE Transactions on Aerospace and Electronic Systems* March 1982; **AES-18**(2):214–218, .

4. Smith WW, Steffes PG. Time delay techniques for satellite interference location system. *IEEE Transactions on Aerospace and Electronic Systems* March 1989; **25**(2):224–231, .

5. Effland J, Gipson JM, Shaffer DB, Webber JC. Method and system for locating an unknown transmitter. US patent US5008679 (A) April 1991.

6. Haworth DP, Smith NG, Bardelli R, Clement T. Interference localization for EUTELSAT satellites-the first European transmitter location system. *International Journal of Satellite Communications and Networking* 1997; **15**(4):155–183, .

7. Grant H, Salt E, Dodds D. Geolocation of communications satellite interference. *2013 26th Annual IEEE Canadian Conference on Electrical and Computer Engineering (CCECE)*, 2013, .

8. Adeogun RO. A robust MUSIC based scheme for interference location in satellite systems with multibeam antennas. *International Journal of Computer Applications* November 2013; **82**(12):1–6, .

9. Fredrick BC. Geolocation of source interference from a single satellite with multiple antennas. Master's Thesis, Naval Postgraduate School, Monterey, California March 2014. URL https://calhoun.nps.edu/handle/10945/41379.

10. Ho D, Chu J, Downey M. Determining transmit location of an emitter using a single geostationary satellite. US patent US8462044 (B1) June 2013.

11. Kalantari A, Maleki S, Chatzinotas S, Ottersten B. Frequency of arrival-based interference localization using a single satellite. *2016 8th Advanced Satellite Multimedia Systems Conference and the 14th Signal Processing for Space Communications Workshop (ASMS/SPSC)*, 2016, .

12. Nölle M. Verfahren zur Identifikation von Störsendern. Austrian patent AT515001 (B1) August 2015.

13. Nölle M. Method for identifying interfering transmitters from a plurality of known satellite transmitters. International patent application WO2015062810 (A1) May 2015.

14. Nölle M. Method for identifying interfering transmitters from a plurality of known satellite transmitters. US patent application US2016254856 (A1) September 2016.

15. Nölle M. Method for identifying interfering transmitters from a plurality of known satellite transmitters. European patent application EP3063879 (A1) September 2016.

16. Nölle M, Ömer B, Suda M. Quantum information algorithms – new solutions for known problems. *e & i Elektrotechnik und Informationstechnik* 2007; **124**(5):154–157, .

17. Nölle M, Suda M. Conjugate variables as a resource in signal and image processing August 2011. URL https://arxiv.org/abs/1108.5720.

18. Nölle M, Suda M, Boxleitner W. H2SI - A new perceptual colour space. *18th International Conference on Digital Signal Processing, DSP 2013, Fira, Santorini, Greece, July 1-3, 2013*, 2013; 1–6, .

19. Bogdanov YI, Bogdanova NA, Lukichev VF, Fastovets DV, Chernyavskii AY. Schmidt decomposition and analysis of statistical correlations. *Russian Microelectronics* 2016; **45**(5):314–323, .

20. Nielsen MA, Chuang IL. *Quantum Computation and Quantum Information: 10th Anniversary Edition*. 10th edn., Cambridge University Press: New York, NY, USA, 2011.

21. Jolliffe I. *Principal Component Analysis*. Springer Series in Statistics, Springer, 2002.

22. Turk MA, Pentland AP. Face recognition using eigenfaces. *Proceedings. 1991 IEEE Computer Society Conference on Computer Vision and Pattern Recognition*, 1991; 586–591, .

AUTHORS' BIOGRAPHIES

Ian Glendinning is a scientist at AIT Austrian Institute of Technology. He specialises in scientific computing, and has worked on applying concepts from quantum information to image and signal processing algorithms, as well as implementing algorithms for scientific applications on Graphics Processing Units (GPUs). Prior to joining AIT Ian worked in High Performance Computing (HPC), focusing primarily on distributed-memory, message-passing systems, and while at the University of Southampton he contributed to standardization in the field through his participation in the design of the MPI Message Passing Interface standard. He then moved to the University of Vienna, where he worked on message-passing software for a range of scientific and commercial applications including satellite signal processing, video indexing, simulation of charged particle optics, and simulation of quantum computers. Ian holds a PhD in experimental high energy particle physics from the University of Manchester.

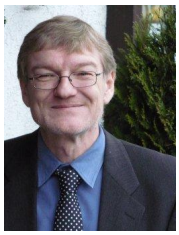

Michael Nölle is a scientist at AIT Austrian Institute of Technology. His current research area is quantum information and image processing, and he has worked on developing quantum inspired algorithms, quantum cryptography, object recognition, content-based image indexing algorithms, image segmentation algorithms, pattern recognition, invariant transformations, benchmarking of image processing systems and video surveillance systems. Prior to joining AIT Michael worked at the University of Technology in Hamburg-Harburg, followed by the Mikroelektronik Anwender Zentrum (MAZ) Hamburg, the University of Vienna, and the University of Freiburg, and during that time he developed fast parallel algorithms with the emphasis on parallel image processing, message-passing systems and communication networks, and portable parallel image processing systems. Michael holds a PhD in computer science from the University of Technology in Hamburg-Harburg.

Christian Hausleitner is Senior Systems Engineer in the ATOS CVC (Atos Convergence Creators GmbH) Satellite Monitoring and Geolocation Solutions unit. He is responsible for system installation, configuration, testing and customer training, as well as focusing on research topics and supporting sales. Prior of joining Atos Space & Avionics, he worked in the Siemens Space business unit dealing with algorithm design, antenna alignment solutions and RF-hardware development, after developing a robust communication system demonstrator based on spread spectrum signals utilizing SAW technology at the Vienna University of Technology (TU Wien), Austria. Christian holds a degree (Master of Science) in Electrical Engineering Telecommunications, from the TU Wien. He is also named as author of several publications and patents dealing with satellite interference geolocation and mitigation solutions as well as passive, wireless sensor design and interrogation systems.

Erwin Greilinger is Sales and Product Line Manager for the Atos CVC (Atos Convergence Creators GmbH) Satellite Monitoring and Geolocation Solutions unit. Thus, he is responsible for the definition of products for monitoring and troubleshooting the quality of satellite communication systems, product marketing as well as technical and commercial sales activities. Prior to joining the Atos Space Business, Erwin was section head for Broadband Management Systems and Fast Internet Solutions. This business sector handled projects in the area of Cross Domain Management Systems especially for Broadband IP and ATM networks. Erwin holds a degree in Electrical Engineering from the Federal Secondary College of Engineering in Vienna, Austria. He is also named as co-author of several patents and has published white papers dealing with satellite interference mitigation solutions.

How to cite this article: I. Glendinning, M. Nölle, C. Hausleitner, and E. Greilinger (20xx), Identification of the source of an interferer by comparison with known carriers using a single satellite, *Int. J. of Satellite Communications and Networking*, *20xx;00:1–6*.